

ADDITIONAL 4-WHEEL STEERING WITH FEEDBACK CONTROL

P. LUGNER and P. MITTERMAYR*

University of Technology, A-1040 Vienna

*Bureau of Applied Mathematics, Lugeck 1-2, A-1010 Vienna

Received: Nov. 10, 1992

Abstract

A computer controlled additional steering of all 4 wheels of a passenger car can be used to correct disturbances much faster than the human driver could do. Based on a complex 4-wheel model and a corresponding tyre model the behaviour of the vehicle in critical situations, especially cornering at μ -split conditions are simulated. Different control schemes, based on the linear 2-wheel model, are compared and their effects evaluated with respect to path deviation and the change of the heading angle. The results show that the introduced feedback control using a reduced observer and a special strategy to identify the μ -split conditions leads to the best corrections. The quality of the control is tested with the cornering on a surface with randomly changing friction.

Keywords: 4-wheel steering, feedback control.

1. Introduction

The actual trends in research and development of passenger cars indicate that the car of the future will have many computer controlled components to improve the vehicle behaviour and its comfort. In the field of active steering — sometimes in combination with traction control — the development of control systems intends to combine better handling quality with improved active safety in critical situations, e.g. [1-6].

The following investigation wants to show possibilities to reduce the path deviations of a vehicle after an instantaneous disturbance. A computer controlled additional steering system can react to such a disturbance much faster than driver will do due to his reaction time lag. Especially at very extreme conditions like the entering of an area of reduced friction during cornering such a system should keep the path deviations to a minimum to present the driver after his reaction time a vehicle as close to the initial or expected condition as possible. For this purpose a feed back control loop with a reduced observer is developed that includes the option to recognize the friction condition qualitatively — if there is a reduced friction at the inner or outer wheel track (μ -split) or at both tracks — and utilize this

information. A comparison of this concept with already investigated or vehicle-tested controls of rear-wheel steering intends to show its advantages.

To get a realistic simulation of the vehicle behaviour itself in this border region of driving, that comprises e.g. locking of wheels, extreme side slip of vehicle and wheels and rapid changing tyre forces, a nonlinear 4-wheel vehicle model with a corresponding tyre description has to be employed. Only by such a complex modelling proper and comparable numerical simulation results can be achieved and the influences of control concepts evaluated. The principal considerations for the control loop of the new concept as well as of the two alternatives are based on the well-known 2-wheel model and the yaw velocity and side slip angle as the main variables of the lateral dynamics.

2. System Modelling

The structure of the system is shown in *Fig. 1* [7]. Because not all essential state variables \mathbf{x} can be measured a reduced observer is employed to provide by the available measurements \mathbf{y} a corresponding estimate $\hat{\mathbf{x}}$. The control vector \mathbf{u} can be modified according to a recognized μ -split condition and finally provides the additional steering wheel angles $\Delta\delta_i$ for all 4 wheels which are added to the driver's steering input δ_F .

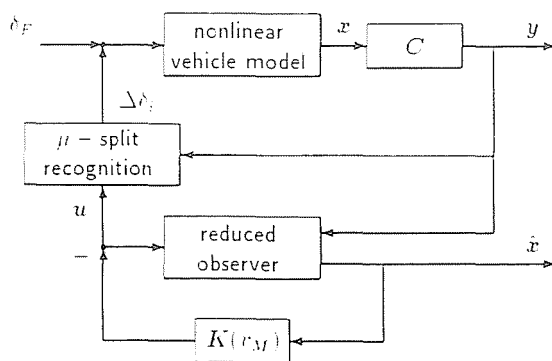


Fig. 1. System structure

The necessary gain matrix \mathbf{K} is determined by the Riccati approach minimizing

$$I = \int_0^{\infty} [\mathbf{x}^T(t)\mathbf{Q}\mathbf{x}(t) + \mathbf{u}^T(t)\mathbf{R}\mathbf{u}(t)] dt \quad (2.1)$$

and using the system equations of the linear 2-wheel model of the observer, see chapter 3. Since the corresponding matrices are functions of the parameter v_M , the running speed \mathbf{K} and its components also vary with v_M .

For the weighting matrices the components are chosen by

$$\begin{aligned} Q_{ii} &= \frac{1}{x_{i, \max}^2}, & Q_{ij} &= 0, \\ R_{ii} &= \frac{1}{u_{i, \max}^2}, & R_{ij} &= 0. \end{aligned} \quad (2.2)$$

Since no actuator system is modelled for the application of the additional steering angles a mathematical limitation of $|\Delta\delta_i| \leq 75^\circ/\text{s}$ is incorporated in the simulation program to avoid unrealistic jumps at immediate changing conditions.

2.1 Nonlinear Vehicle Model

The chosen 4-wheel model is described in detail in [6] and only the essential characteristics will be stated for the understanding of the results.

The description is chosen in such a way that the features essential for this investigation could be described to the full extent. Components or characteristics that may lead to effects rather disturbing for the interpretation of the main influences are simplified or idealized. For the environment calm air and flat horizontal road with suddenly changing surface conditions are presupposed.

The scheme of the vehicle model, *Fig. 2*, shows the selected state variables, roll angle φ , pitch angle ν , heave h , yaw angle ψ , side slip angle β and longitudinal velocity v_M of the reference point M . The normal tyre force F_{z_i} for wheel i is calculated using the wheel travel $f_i = f_i(\varphi, \nu, h)$ and its derivative to determine the nonlinear spring and damper force of the suspension.

To suppress the self steering and other effects of the wheel suspensions, it is assumed that the wheel planes are always normal to the road surface. So the steering of a wheel is only caused by the driver's action — presented by δ_F due to a parallel steering for large radii — and/or the additional steering angles $\Delta\delta_i$ of the control system.

For the vehicle aerodynamics only the essential quantities, drag force W_x , lateral force W_y and a yaw moment M_u with respect to the center of the vehicle body are taken into account.

To be able to calculate the individual wheel spin velocities ω_i of each wheel the drive train is modelled as a 4-wheel drive with engine character-

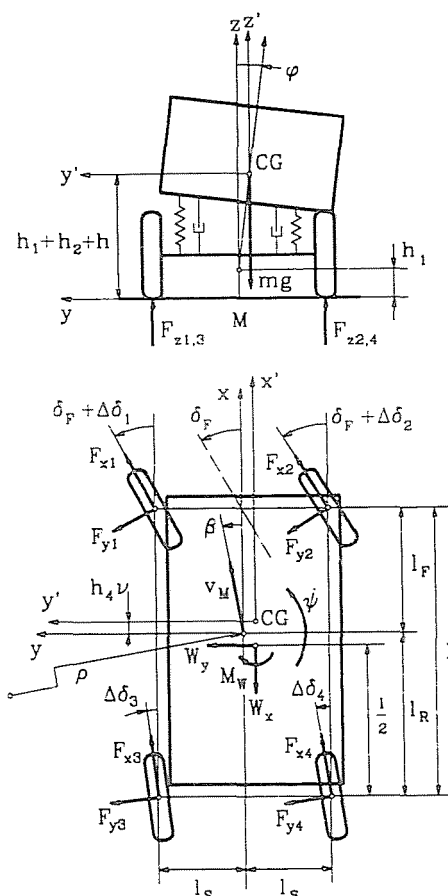


Fig. 2. Scheme of vehicle model

istics, unlocked central differential and axle differentials. Besides the common brake moment distribution front to rear wheels different additional braking moments ΔM_{B_i} can be applied at each of the wheels.

For the description of the behaviour by the steady state characteristics of the longitudinal force $F_{x_i}^s$ and the lateral force $F_{y_i}^s$ an approximation partially similar to the 'magic formula' was chosen [8]. It includes large slip values in longitudinal s_{L_i} and lateral direction (side slip angle of the wheel α_i) and therefore comprises the whole possible range of force transfer between tyre and road surface, Fig. 3. Moreover, due to a simple change of 3 parameters a change of surface conditions can be described.

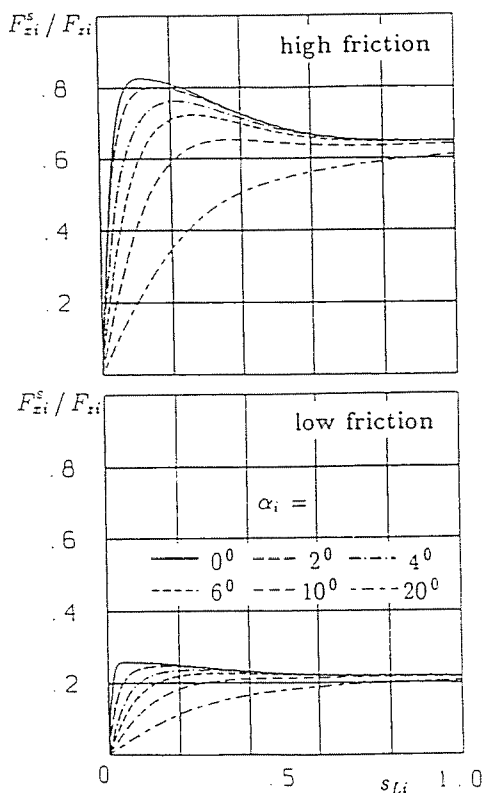


Fig. 3. Steady state tyre characteristics for two different friction conditions; normal force F_{zi} = constant

Since only the steering angles of the wheels are modelled as a substitute for the steering system, the tyre self aligning torque and its insignificant effects on the overall vehicle motion are omitted.

Due to the rapid changes in the surface conditions it is necessary for the simulation to consider the transition tyre behaviour. The common description in the form of a first order differential equation is used for the lateral and longitudinal tyre forces

$$\dot{F}_{yi} = \frac{v_{Li}}{l_{yi}} (F_{yi}^s - F_{yi}) , \quad \dot{F}_{xi} = \frac{v_{Li}}{l_{xi}} (F_{xi}^s - F_{xi}) . \quad (2.3)$$

The constant transitional length for F_{xi} is assumed $l_{xi} = 0.25$ m and that of the lateral force F_{yi} with $l_{yi} = 0.3$ m.

2.2 2-Wheel Model for Controller Design

The control strategies considered are based on the representation of the vehicle by a linear 2-wheel model, *Fig. 4*. This model is well known and documented, e.g. [10–11].

The essential equations with the nomenclature corresponding to *Fig. 2* are (with the vehicle mass m and moment of inertia Θ_z with respect to the vertical axis)

$$\dot{\beta} = A_{11}\beta + A_{12}\dot{\psi} + \sum_{i=1}^4 B_{1i}\Delta\delta_i + \frac{2C_F}{mv_M}\delta_F, \quad (2.4)$$

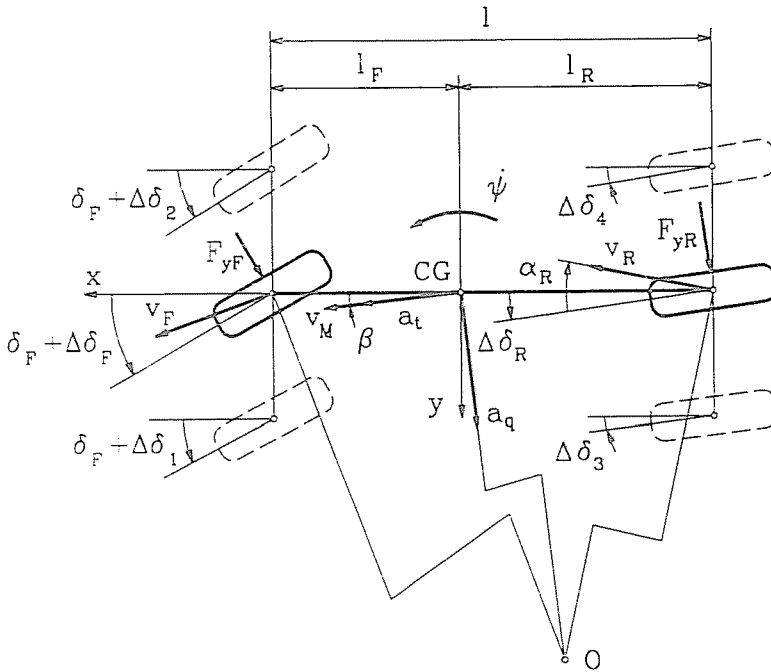


Fig. 4. Linear 2-wheel model

$$\ddot{\psi} = A_{21}\beta + A_{22}\dot{\psi} + \sum_{i=1}^4 B_{2i}\Delta\delta_i + \frac{2C_F}{\Theta_z}l_F\delta_F, \quad (2.5)$$

with the elements of the system matrix A

$$\begin{aligned}
 A_{11} &= -\frac{2C_F + 2C_R}{mv_M}, \\
 A_{12} &= -1 - \frac{2C_F l_F - 2C_R l_R}{mv_M^2}, \\
 A_{21} &= -\frac{2C_F l_F - 2C_R l_R}{\Theta_z}, \\
 A_{22} &= -\frac{2C_F l_F^2 + 2C_R l_R^2}{\Theta_z v_M}
 \end{aligned}
 \tag{2.6}$$

and the control matrix

$$\begin{aligned}
 B_{1i} &= \frac{C_F}{mv_M}, & B_{2i} &= \frac{C_F l_F}{\Theta_z}, & i &= 1, 2, \\
 B_{1i} &= \frac{C_R}{mv_M}, & B_{2i} &= -\frac{C_R l_R}{\Theta_z}, & i &= 3, 4.
 \end{aligned}
 \tag{2.7}$$

The formulations of (2.4), (2.5), (2.7) allow to consider an individual additional steering $\Delta\delta_i$ at every wheel.

The constant cornering stiffness C_F for one front wheel and C_R for one rear wheel, respectively are determined approximately by the side slip values α_i and the lateral forces F_i of the steady state cornering nonlinear vehicle model

$$C_F = \left(\frac{F_{y1} + F_{y2}}{\alpha_1 + \alpha_2} \right), \quad C_R = \left(\frac{F_{y3} + F_{y4}}{\alpha_3 + \alpha_4} \right).
 \tag{2.8}$$

Using for this investigation the initial undisturbed steady state cornering, the approximation (2.8) leads to better results than the definition of C_F , C_R as cornering stiffnesses derived from tyre characteristics at $\alpha = 0$.

The lateral acceleration a_q of the CG of the 2-wheel model can be expressed by the two system variables in the form

$$a_q = v_M(\dot{\beta} + \dot{\psi}).
 \tag{2.9}$$

For the steady state cornering without additional steering ($\Delta\delta_i = 0$) the yaw velocity can be calculated using (3.1) with

$$\dot{\psi}_{stat} = \frac{v_M}{l + \frac{mv_M^2(C_R l_R - C_F l_F)}{2C_F C_R l}} \delta_F.
 \tag{2.10}$$

Since all 4 additional steering angles $\Delta\delta_i$ are included in the formulation (2.4) to (2.7), more than necessary to control the lateral dynamics, there are further options available to define additional interrelations.

The most commonly used rear wheel steering, described by

$$\Delta\delta_1 = \Delta\delta_2 = 0, \quad \Delta\delta_3 = \Delta\delta_4 = \Delta\delta_R = \delta_R, \quad (2.11)$$

uses only one quantity $\Delta\delta_R$ for the control.

More efficiency in correcting disturbances offers an employment of two control variables $\Delta\delta_R$ and $\Delta\delta_F$, e.g. in the form of

$$\Delta\delta_1 = \Delta\delta_2 = \Delta\delta_F, \quad \Delta\delta_3 = \Delta\delta_4 = \Delta\delta_R = \delta_R. \quad (2.12)$$

Supposing that the car body accelerations $a_y \equiv a_q$ and $a_x \equiv a_t$ of the CG are measured and the rolling stiffness ratio of the vehicle suspension is known, the normal forces F_{zi} can be determined approximately [6] and then used to find a weighted distribution:

$$\begin{aligned} \Delta\delta_i &= \Delta\delta_F \frac{2F_{zi}}{F_{z1} + F_{z2}}, & i = 1, 2, \\ \Delta\delta_i &= \Delta\delta_R \frac{2F_{zi}}{F_{z3} + F_{z4}}, & i = 3, 4. \end{aligned} \quad (2.13)$$

When a μ -split condition can be recognized and the track with lower friction identified — see chapter 5 — the additional steering can be adjusted with

$$\begin{aligned} \Delta\delta_i &= 2\Delta\delta_{F,R} && \text{high friction side} \\ \Delta\delta_i &= 0 && \text{low friction side} \end{aligned} \quad (2.14)$$

to use the friction capacity best.

3. Reduced Observer

Since today the side slip angle β of the vehicle cannot be measured without very special measuring equipment, a main purpose of the reduced observer is to provide a good estimate of β based on the easy available lateral acceleration a_y of the car body (2.9).

For the mathematical description of the reduced observer with the steady state cornering as a reference *Eqs.* (2.4), (2.5) can be written in the form

$$\dot{\mathbf{x}}(t) = \mathbf{A}\mathbf{x}(t) + \mathbf{B}\mathbf{u}(t), \quad (3.1)$$

$$\mathbf{x}^T = [\Delta\beta, \Delta\dot{\psi}], \quad \mathbf{u}^T = [\Delta\delta_F, \Delta\delta_R]. \quad (3.2)$$

The elements of the Matrix **A** are given by (2.6) whereas for the observer design those of **B** are calculated by (2.7) and (2.12). The state vector **x** comprises the changes of the state variables with respect to their steady state values. Therefore driver's steering angle δ_F does not appear in (3.1).

The general form of the measurements is given by

$$\mathbf{y}(t) = \mathbf{C}\mathbf{x}(t) + \mathbf{D}\mathbf{u}(t). \quad (3.3)$$

With the measured lateral acceleration

$$y(t) = \Delta a_y \equiv \Delta a_q = v_M(\Delta\dot{\beta} + \Delta\dot{\psi}), \quad (3.4)$$

and elimination of $\dot{\beta}$ with the help of (2.4) the two matrices can be found with

$$\mathbf{C}^T = \begin{bmatrix} A_{11}v_M \\ (A_{12} + 1)v_M \end{bmatrix}, \quad \mathbf{D}^T = \begin{bmatrix} (B_{11} + B_{12})v_M \\ (B_{13} + B_{14})v_M \end{bmatrix}. \quad (3.5)$$

Using now equations (3.1), (3.2), (3.3) a reduced observer [12, 7] is chosen starting with

$$\dot{\mathbf{z}} = \mathbf{F}\mathbf{z} + \mathbf{B}_t\mathbf{u} + \mathbf{H}\mathbf{y} \quad (3.6)$$

and the observer error

$$\mathbf{e} = \mathbf{z} - \mathbf{T}\mathbf{x}. \quad (3.7)$$

The transient response of this error

$$\dot{\mathbf{e}} = \mathbf{F}\mathbf{e} + (-\mathbf{T}\mathbf{A} + \mathbf{F}\mathbf{T} + \mathbf{H}\mathbf{C})\mathbf{x} + (\mathbf{B}_t - \mathbf{T}\mathbf{B} + \mathbf{H}\mathbf{D})\mathbf{u} \quad (3.8)$$

shows that with the additional conditions

$$\mathbf{T}\mathbf{A} - \mathbf{F}\mathbf{T} = \mathbf{H}\mathbf{C}, \quad \mathbf{B}_t = \mathbf{T}\mathbf{B} - \mathbf{H}\mathbf{D} \quad (3.9)$$

and selecting a matrix **F** with negative real parts of its eigenvalues, **e** will asymptotically go to zero. Therefore, assuming no further disturbances, for the stationary case the estimated value $\hat{\mathbf{x}}$ of the state vector **x** is, see also *Fig. 5*:

$$\hat{\mathbf{x}} = \begin{bmatrix} \mathbf{C} \\ \mathbf{T} \end{bmatrix}^{-1} \begin{bmatrix} \mathbf{y} - \mathbf{D}\mathbf{u} \\ \mathbf{z} \end{bmatrix}. \quad (3.10)$$

In the considered case of one measurement and two estimated variables, **z** and **F** are scalars. The eigenvalue of **F** is chosen with $\lambda_F = -75 \text{ s}^{-1}$ to have a quick decreasing of the observer error. Choosing further the first component of **T** with $T_1 = 1 \text{ Eqs.}$ (3.9) determine the scalar **H** and the matrix **B_t**.

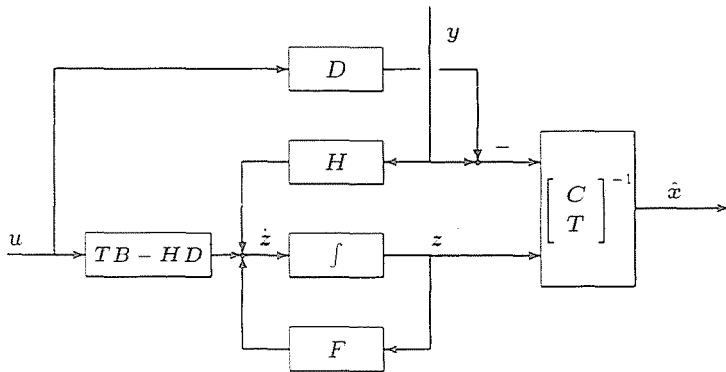


Fig. 5. Scheme of reduced observer

4. Alternative Control Strategies

To make easier evaluating the effects of the reduced observer together with the μ -recognition a comparison with two other rear wheel steering concepts is shown. Both of these established concepts are also based on the linear 2-wheel model of Chapter 2.

The rear wheel steering with yaw-velocity feedback of SATO et al. [13] (further in the results marked SATO), determines the steering angle δ_R of the rear wheels by

$$\delta_R = -\delta_F + C_2 v_M \dot{\psi} \quad (4.1)$$

with the constant gain

$$C_2 = \left(\frac{l_R}{2C_F} + \frac{l_F}{2C_R} \right) \frac{m}{2l}. \quad (4.2)$$

This kind of control has the intention to keep the side slip angle β of the vehicle at zero. (4.1) and (4.2) guarantee this compensation for the linear vehicle, Fig. 4, with $l_F = l_R$.

The yaw-velocity feedback control, implemented in the VW research vehicle Futura (further marked FUTURA), uses the steady state yaw velocity (3.6) as a reference [14]:

$$\delta_R = k_{\dot{\psi}} (\dot{\psi} - \dot{\psi}_{\text{stat}}) \quad (4.3)$$

and thereby compensates disturbances with respect to an ideal steady state behaviour. There are given 2 values for the constant gain: $k_{\dot{\psi}} = 0.28$ for moderate and $k_{\dot{\psi}} = 1.4$ for sporty driving. The lower value was chosen for the evaluations in Chapter 5.

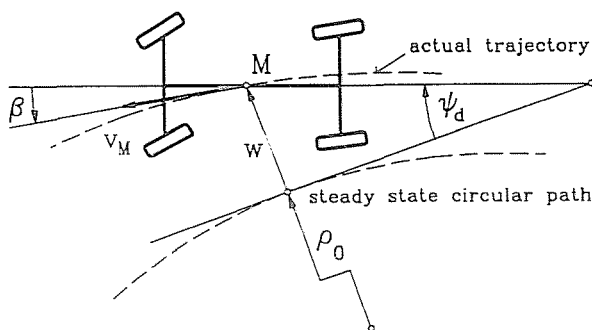


Fig. 6. Characterization of path deviation by distance w and angle ψ_d

5. Simulation and Results

For the evaluations the data according to a medium size passenger car with permanent all-wheel drive are used. The main characteristics are

$$\begin{aligned}
 m &= 1360 \text{ kg}, & l &= 2.6 \text{ m}, & \frac{(h_1 + h_2)}{l} &= 0.2, \\
 \Theta_z &= 2300 \text{ kgm}^2, & \frac{l_F}{l} &= 0.5, & \frac{2l_s}{l} &= 0.52,
 \end{aligned}$$

The components of the weighting matrices (2.2) are chosen with

$$\begin{aligned}
 x_{1,\max} &= \beta_{\max} = 0.25^\circ, & u_{1,\max} &= \Delta\delta_{F,\max} = 5^\circ, \\
 x_{2,\max} &= \dot{\psi}_{\max} = 0.1 \text{ s}^{-1}, & u_{2,\max} &= \Delta\delta_{H,\max} = 5^\circ.
 \end{aligned}$$

For the necessary sensor signals, it is assumed that the longitudinal acceleration $a_t \cong a_x$ and the lateral acceleration $a_q \cong a_y$ of the CG of the body are available. Furthermore, the wheel spin velocities ω_i are used to recognize the μ -split condition.

The steering input δ_F and the acceleration pedal position are assumed to be constant (corresponding to their steady state values) during the whole considered motion. At the beginning the vehicle performs a steady state cornering (characterized by the lateral acceleration a_{q0}) with a radius $\rho_0 = 50 \text{ m}$. After a short distance, the vehicle encounters changed surface conditions.

The thereafter starting deviations from circular trajectory are characterized by the deviation angle ψ_d and the distance w , Fig. 6. The angle ψ_d is set to zero for the steady state starting condition by subtracting the initial value β_0 .

For the calculation process itself, the steady state initial condition is provided by an iteration whereas the following behaviour is the result of a distance related integration.

The different surface conditions are characterized with the maximum contact force coefficient μ_{\max} :

$$\begin{aligned} \text{high friction:} & \quad \mu_{\max} \cong 0.85, \\ \text{tracks low friction:} & \quad \mu_{\max} \cong 0.45, \\ \text{low friction (for } \mu\text{-split):} & \quad \mu_{\max} \cong 0.25. \end{aligned}$$

In *Fig. 3* the tyre characteristics correspond to $\mu_{\max} \cong 0.85$ and $\mu_{\max} \cong 0.25$, respectively.

Besides the step-like change but otherwise homogeneous surface a random variation of μ_{\max} is considered also to have a more severe condition to test the μ -split recognition and the quality of the reduced observer.

Therefore a random input signal is created, assuming a spectral density [9]

$$\Phi_{\mu}(\Omega) = \Phi_{\mu}(\Omega_0) \left(\frac{\Omega}{\Omega_0} \right)^{-2} \quad (5.1)$$

equivalent to the commonly used road roughness descriptions with Ω being the spatial angular frequency. Using (5.1) and the driving velocity a time description can be established [9, 14].

For the random fluctuations of the maximum contact force coefficient for left and right track

$$\begin{aligned} \bar{\mu}_L &= \sum_i \bar{\mu}_{L_i} = \sum_i c_i \sin(\omega_i t + \varphi_{L_i}), \\ \bar{\mu}_R &= \sum_i \left(\gamma_i \bar{\mu}_{L_i} + \sqrt{1 - \gamma_i^2} c_i \sin(\omega_i t + \varphi_{R_i}) \right) \end{aligned} \quad (5.2)$$

the factors c_i can be calculated by (5.1) whereas the phase angles φ_{L_i} , φ_{R_i} are determined by random numbers. The parameters γ_i characterize the cross correlation of left and right track.

Superimposing (5.2) on the μ -split surface leads to the randomly changing μ_{\max} of both tracks shown in *Fig. 7*. To cope with problems of different surface qualities, three different RMS-values of the random input are considered.

With respect to the μ -split recognition — details are given in [7] — only the essential features will be explained.

When the car enters the μ -split or reduced friction area first with the front wheels and later with the rear wheels according to these events there will be two distinct declines in the lateral acceleration. Since they

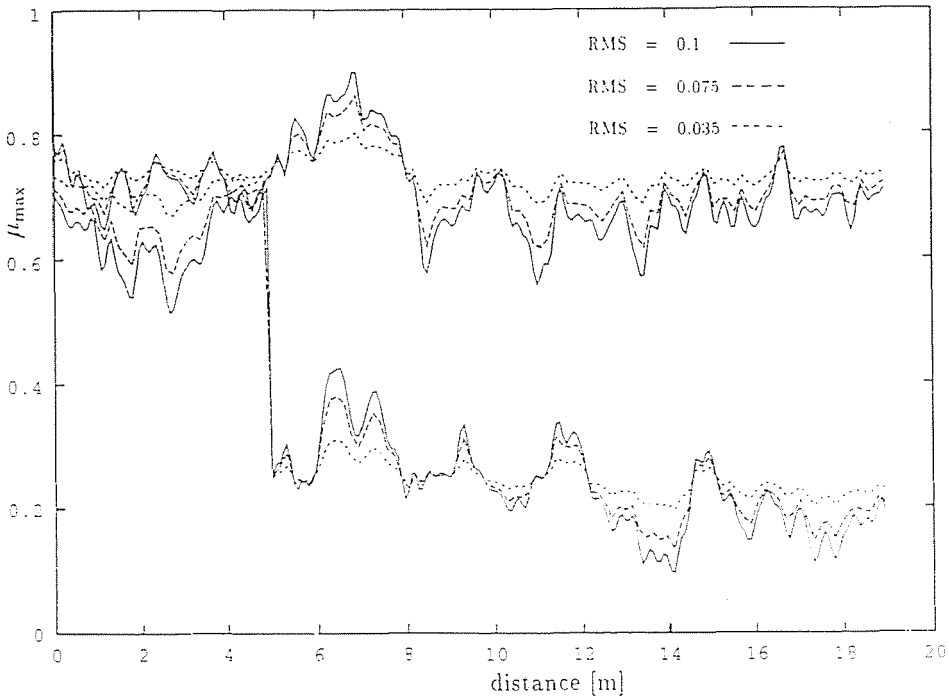


Fig. 7. Maximum contact force coefficients of left and right track with random fluctuations and μ -split

are spaced due to driving speed and wheel base, after the first decline a recognition window can be set, that allows an identification of the second, wheel base related acceleration decline. In this way the disturbances are identified to be determined by the road surface conditions. A short controlled braking of the front wheels after such an identification results in changes of the spin velocities ω_1, ω_2 . The sign of the change of difference of $\omega_1 - \omega_2$ provides the information if the outer or inner wheel tracks have the lower friction or if there are only negligible differences.

For a cornering on a road with random μ_{max} values and μ -split Fig. 8 shows the changes in lateral acceleration a_q and its numerically determined derivative \dot{a}_q used for the identification. If the variance of the random changes is below a special value, the entering of the surface condition change is detected. In this case the additional braking of the front wheels leads to a short decrease in the lateral acceleration a_t and an increase in difference in the wheel spin velocities. The latter indicates the lower friction at the

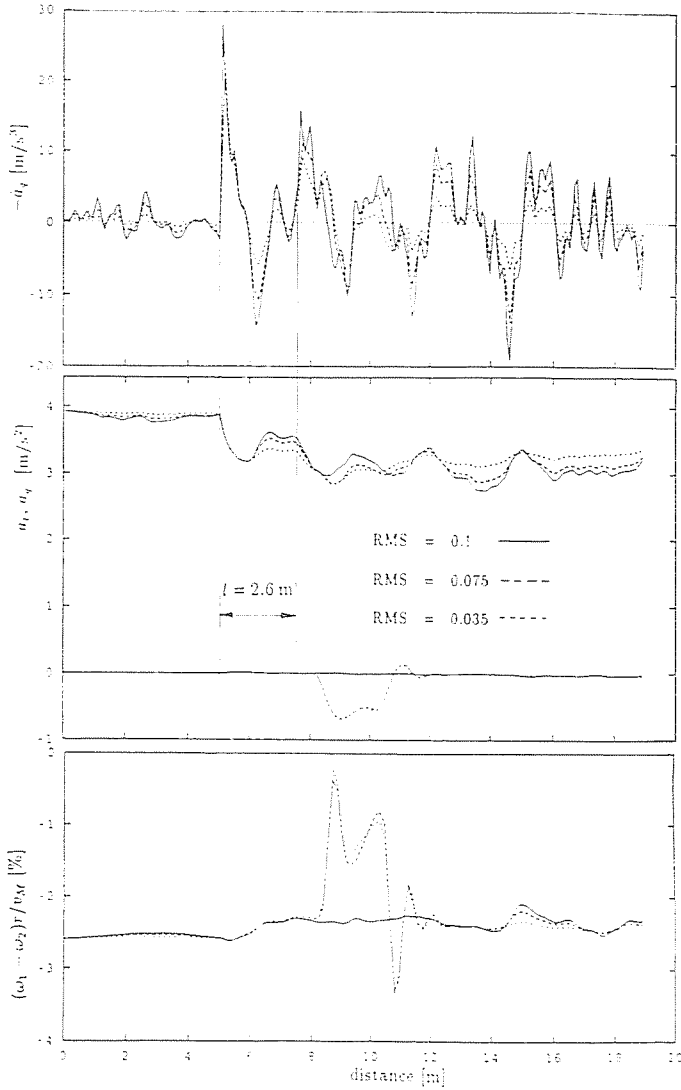


Fig. 8. Changes of lateral acceleration a_q due to surface Fig. 7 and the consequences of additional braking of both front wheels

track of wheel 2 by a greater decline of ω_2 compared to ω_1 though the same braking moments are applied.

When no recognition is possible, the feedback control is still active but it only does not make use of a distribution of the additional steering angles due to μ -split friction (2.14) but provides the additional steering

weighted with the normal forces (2.13). If a surface change is detected but the additional braking leads to no essential differences in the changes of $\omega_1 - \omega_2$ the strategy (2.14) for low friction outer track is applied.

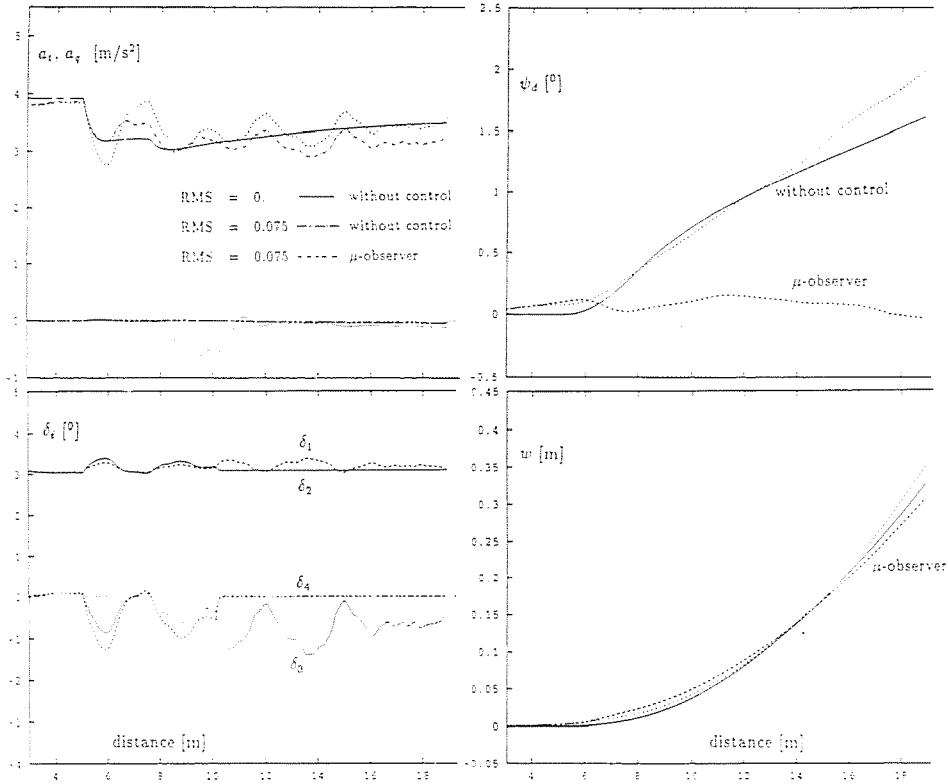


Fig. 9. Comparison of a vehicle with and without control, random surface Fig. 7 with low friction outer track

In Fig. 9 a comparison of the vehicle on homogeneous surface with μ -split, is demonstrated low friction outer track and with additionally random disturbances. While the uncontrolled vehicle shows increasing deviations for both surface conditions in the second case the controlled vehicle (reduced observer together with μ -split recognition: named ' μ -observer') shows only minimal deviation angles ψ_d while the improvement in lateral deviation w becomes obvious only with longer running distance.

The following results and comparisons are calculated for homogeneous friction conditions only.

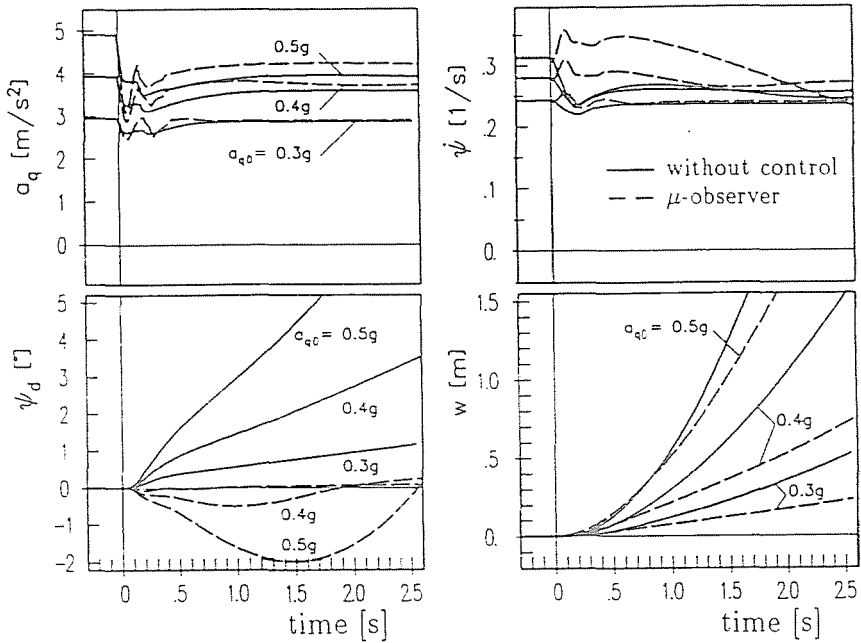


Fig. 10. Low friction outer track: influences of the initial lateral acceleration a_{q0}

The range of possible improvements by the reduced observer plus μ -recognition set by the physical limits becomes clear by Fig. 10. When the initial lateral acceleration a_{q0} is too high, even a very good feedback control can only lead to small improvements. On the other hand, for low a_{q0} a disturbance due to μ -split, low friction outertrack results in only small deviations in w and ψ_d even for the uncontrolled vehicle. Therefore the case of $a_{q0} = 0.4g$ was selected for the further investigations.

The consequences of the different control concepts are compared in Fig. 11. With respect to the vehicle without control the SATO control and the FUTURA control show nearly the same quantitative improvements though they are not designed for such extreme conditions. A further remarkable improvement can be achieved with the use of the ' μ -observer'. All three concepts need additional rear wheel steering angles δ_3 , δ_4 of about the same size. The changes of the frontwheel steerangles δ_1 , δ_2 for the μ -observer show that the corresponding $\Delta\delta_1$, $\Delta\delta_2$ are very small and even at the beginning of the disturbance less than 0.5° . For the change $\Delta\beta$ of the slip angle β with respect to its initial value all concepts show larger values than the vehicle without control, though these values are still absolutely small. Here the μ -observer provides the largest differences in the

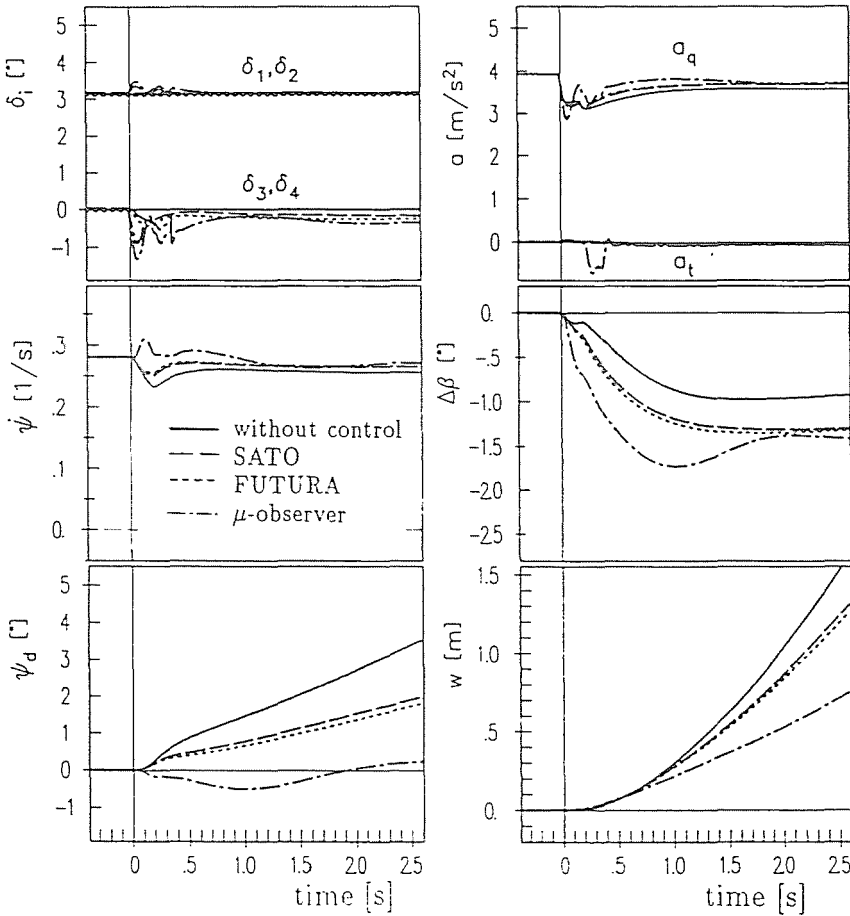


Fig. 11. Low friction outer track: comparison of different control concepts

first period. The changes in lateral acceleration a_q and yaw velocity $\dot{\psi}$ show comparable patterns to the $\Delta\beta$ -diagram.

Corresponding to Fig. 11 in Fig. 12 the results of the control concepts are shown in the case when the inner and outer wheels encounter lower friction ($\mu_{max} \sim 0.4$). Though now the μ -recognition leads to the same reaction of the μ -observer like with low friction outer track only the improvements are absolutely and relatively similar to that of Fig. 12. The same holds for the SATO and FUTURA control. The only obvious difference is with $\Delta\beta$: here the μ -observer finally reaches a lower value than the other two control concepts. Once again the advantages of the μ -observer are clearly obvious.

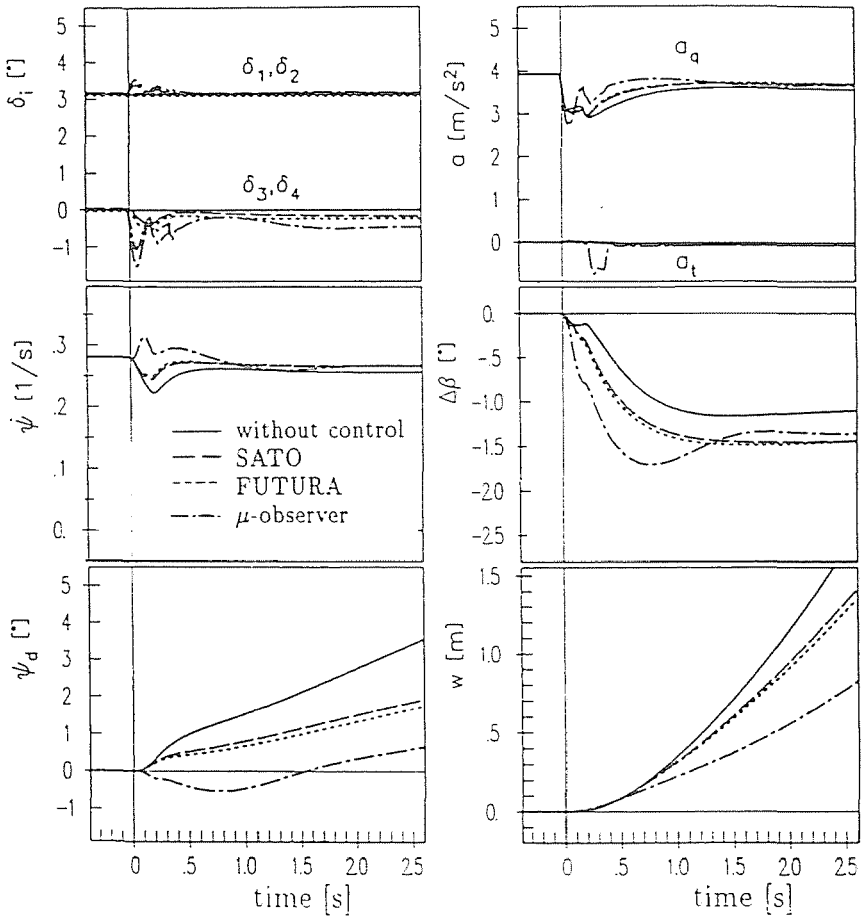


Fig. 12. Lower friction both tracks: corresponding diagrams to Fig. 11

In the case of μ -split low friction at the inner track the consequences for the vehicle behaviour are qualitatively the same like those in Fig. 12 but of smaller amount. A deviation $w \cong 0.55$ m at $t = 2$ s for the uncontrolled vehicle is reduced to about 0.4 m for the FUTURA and SATO control concepts but to about 0.2 m with the μ -observer, the corresponding deviation angle $\psi_d \sim 1.3^\circ$ to about 0.5° and -0.1° , respectively.

6. Conclusions

Starting with the considerations to develop a strategy that should increase the active safety in the reaction time of the driver a feedback control for an additional 4-wheel steering was introduced.

The results of the investigations of very critical situations show encouraging improvements with the chosen reduced observer and μ -split recognition scheme. Though it is neither the intention nor it is possible by this concept to fully compensate the changed surface conditions the reduction in deviation angle and deviation distance with respect to the undisturbed circular trajectory will support the driver to bring the vehicle back to the desired path.

References

1. ABE, M.: Handling Characteristics of Four-wheel Active Steering Vehicles Over Full Manoeuvring Range of Lateral and Longitudinal Accelerations. *Proc. of the 11th IAVSD Symposium*, Canada, 1989, Swets & Zeitlinger, 1990.
2. DONGES, E. – AUFFHAMMER, R. – FEHRER, P. – SEIDENFUSS, T.: Funktion und Sicherheitskonzept der aktiven Hinterachskinematik von BMW. *ATZ* 92, 1990.
3. FURUKAWA, Y. – YUHARA, N. – SANO, S. – TAKEDA, H. – MATSUSHITA, Y.: A Review of Four-wheel Steering Studies from the Viewpoint of Vehicle Dynamics and Control. *Vehicle System Dynamics*, Vol. 18, 1989.
4. YAMAMOTO, M. – HARADA, H. – MATSUI, Y.: A Study on Active Controlled Chassis System for Vehicle Dynamics. *Proc. of the 11th IAVSD Symposium*, Canada, 1989, Swets & Zeitlinger, 1990.
5. WALLENTOWITZ, H.: Aktive Fahrwerkstechnik. *Fortschritte der Fahrzeugtechnik*, Band 10, Vieweg-Verlag, 1991.
6. LUGNER, P. – MITTERMAYR, P.: Possibilities to Improve the Vehicle Cornering Dynamics by the Control of the Tyre Forces. *Proc. of the 11th IAVSD Symposium*, Canada, 1989, Swets & Zeitlinger, 1990.
7. LUGNER, P. – MITTERMAYR, P.: Controlled Additional 4-Wheel Steering at Critical Driving Conditions. *Proceedings of the AVEC'92 Symposium, Society of Automotive Engineers of Japan (JSAE)*, 1992.
8. LUGNER, P. – MITTERMAYR, P.: A Measurement Based Tyre Characteristics Approximation. *Proceedings of the 1st International Colloquium on Tyre Models for Vehicle Dynamics Analysis*, 1991, Swets & Zeitlinger, in press.
9. MITSCHKE, M.: Dynamik der Kraftfahrzeuge, Band B: Schwingungen. Springer Verlag, Berlin, Heidelberg, New York, 1984.
10. MITSCHKE, M.: Dynamik der Kraftfahrzeuge, Band C: Fahrverhalten. Springer Verlag, 1990.
11. SHARP, R. S. – CROLLA, D. A.: Controlled Rear Steering for Cars — a Review. *International Conference 'Advanced Suspensions'*, *IMechE* 9/1988.
12. HIPPE, P. – WURMTHALER, CH.: Zustandsregelung. Springer Verlag, 1985.
13. SATO, H. – HIROTA, A. – YANAGISAWA, H. – FUKUSHIMA, T.: Dynamical Characteristics of a Whole Wheel Steering Vehicle with Yaw Velocity Feedback Rear Wheel Steering. *IMechE* C124/83, 1983.
14. RICHTER, B.: Schwerpunkte der Fahrzeugdynamik. Verlag TÜV Rheinland, 1990.